International Center
Institute of Applied Optics
National Academy of
Sciences of Ukraine

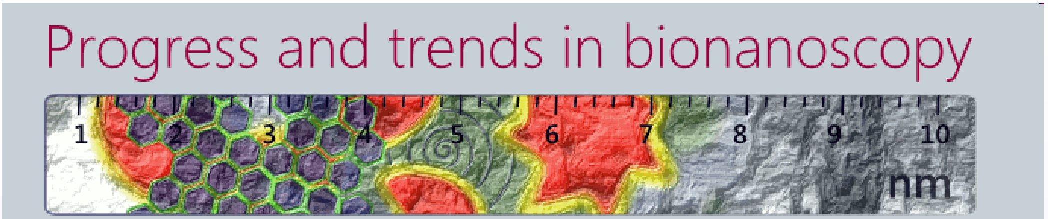

AFM-investigation of ion-implanted channels in diamond-based biosensor

Oksana Budnyk

4th International Conference, 15-18th June 2010, Moscow

What is a biosensor?

Biosensor as a device

Converts biological information into physical one

Living cells as sensor elements

They have a **high sensitivity** to a broad range of biologically active substances.

They offer **variation** of the **physiochemical** (temperature, pH, ion concentration....) and **physiological** (growth factor, hormones....) **environments**.

Why is it important to have a cell-based biosensor?

Because there are many promising fields for potential use of cell-based biosensors:

- Environmental monitoring (chemical/biological warfare agents, groundwater contamination...),
- Pharmaceutical screening,
- Drug discovery,
- Basic neuroscience

Ideal bio-sensing substrate

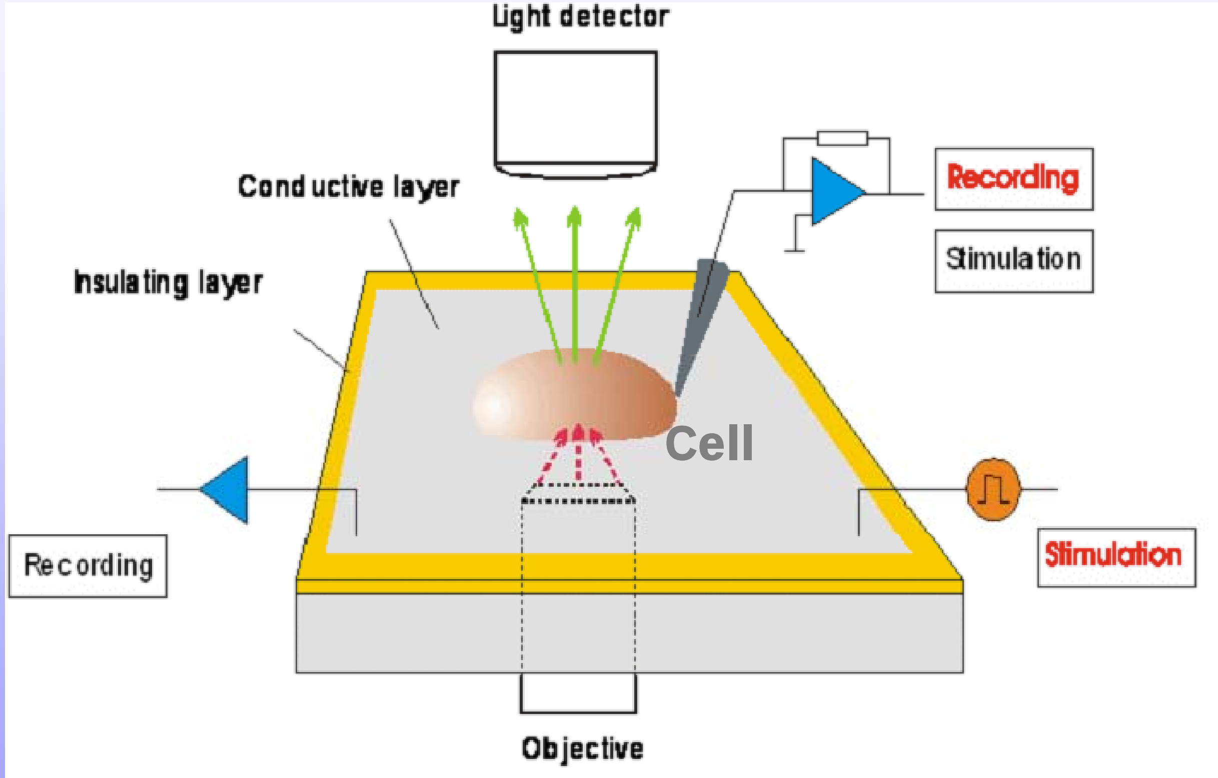

What is the material that can combine next properties:

- **Transparency**
- **Surface functionalization**
- **Surface conductivity**
- **Biocompatibility**

?

Diamond

The crystal structure of diamond is equivalent to a face-centred cubic (FCC) lattice.

The conventional unit cell is cubic with a side length a_0 approximately equal to 3.567 Å at room temperature.

The C – C bond length *d* is equal to 1.54 Å. The atomic density is 1.76×10^{23} atoms/cm^3.

Its covalent bonds between hybrid sp^3 orbitals make it the hardest material in nature

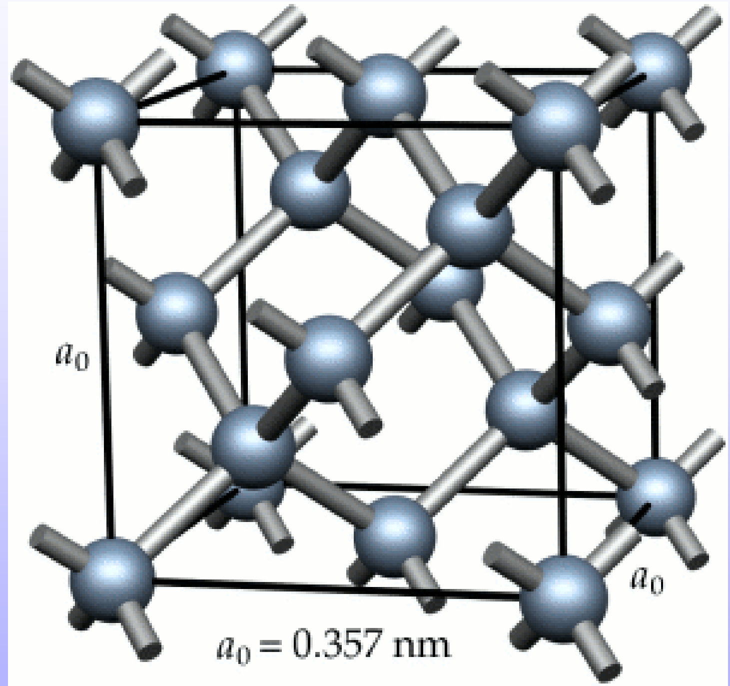

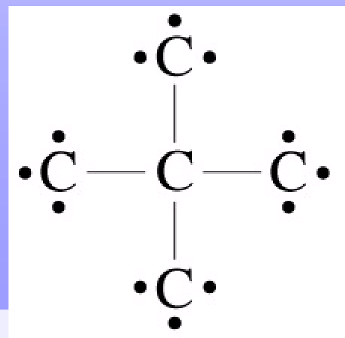

Diamond Surface

Clean surface

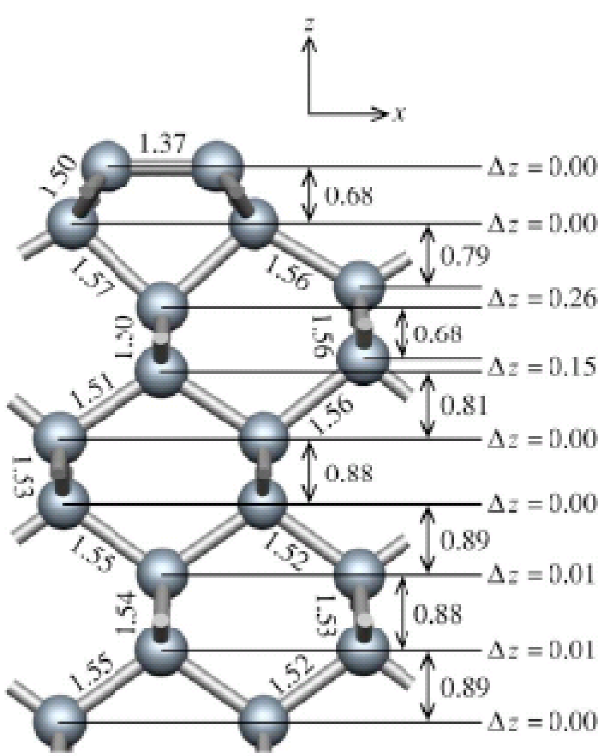

Clean

Face (100) properties

Without adsorbates:

C symmetrical dimers, linked together with double bond (σ,π)

With (single) H:

C atoms arranged as dimers, but only with σ bonds, while an H atom terminates the dangling bond

H - terminated

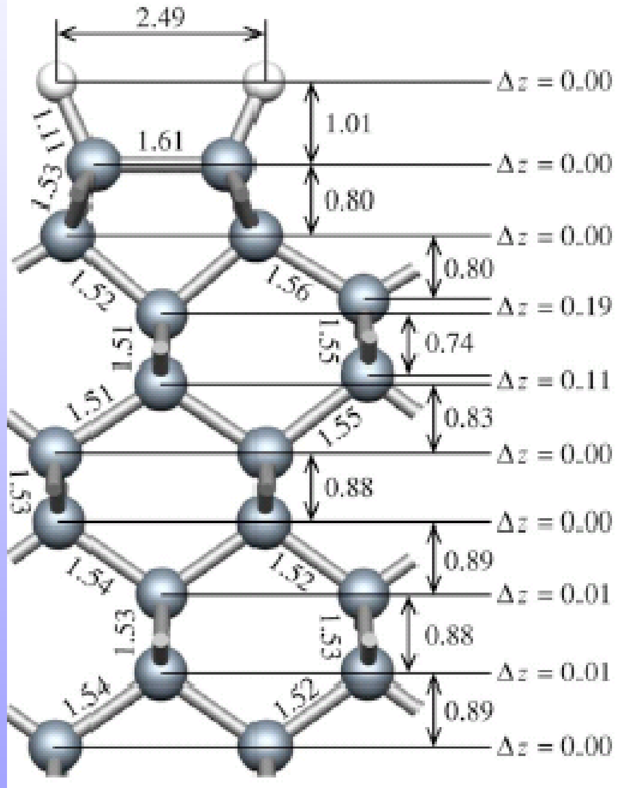

Hydrogenated

*S. J. Sque et al. - Physical Rev B **73**, 2006*

Microelectrodes

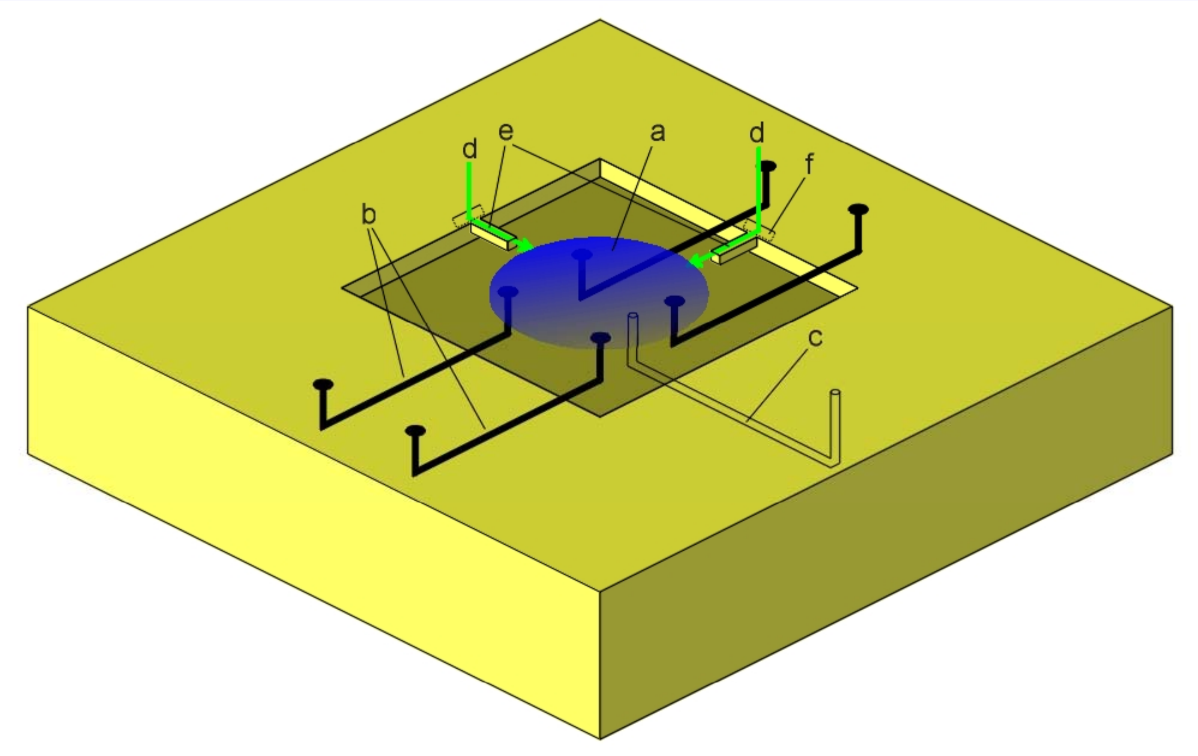

To realize a diamond lab-on chip
we need a technique able to micromachine diamond

The components of diamond-based sensor device are:

a: cell
b: graphitic conductive paths
c: microfluidic channel
d: laser beams
e: optical micro-probes

In order to make **integrated cell biosensor** (for creation scaffolds where cell to be located or make buried conductivity channels)

MeV ion implantation technique

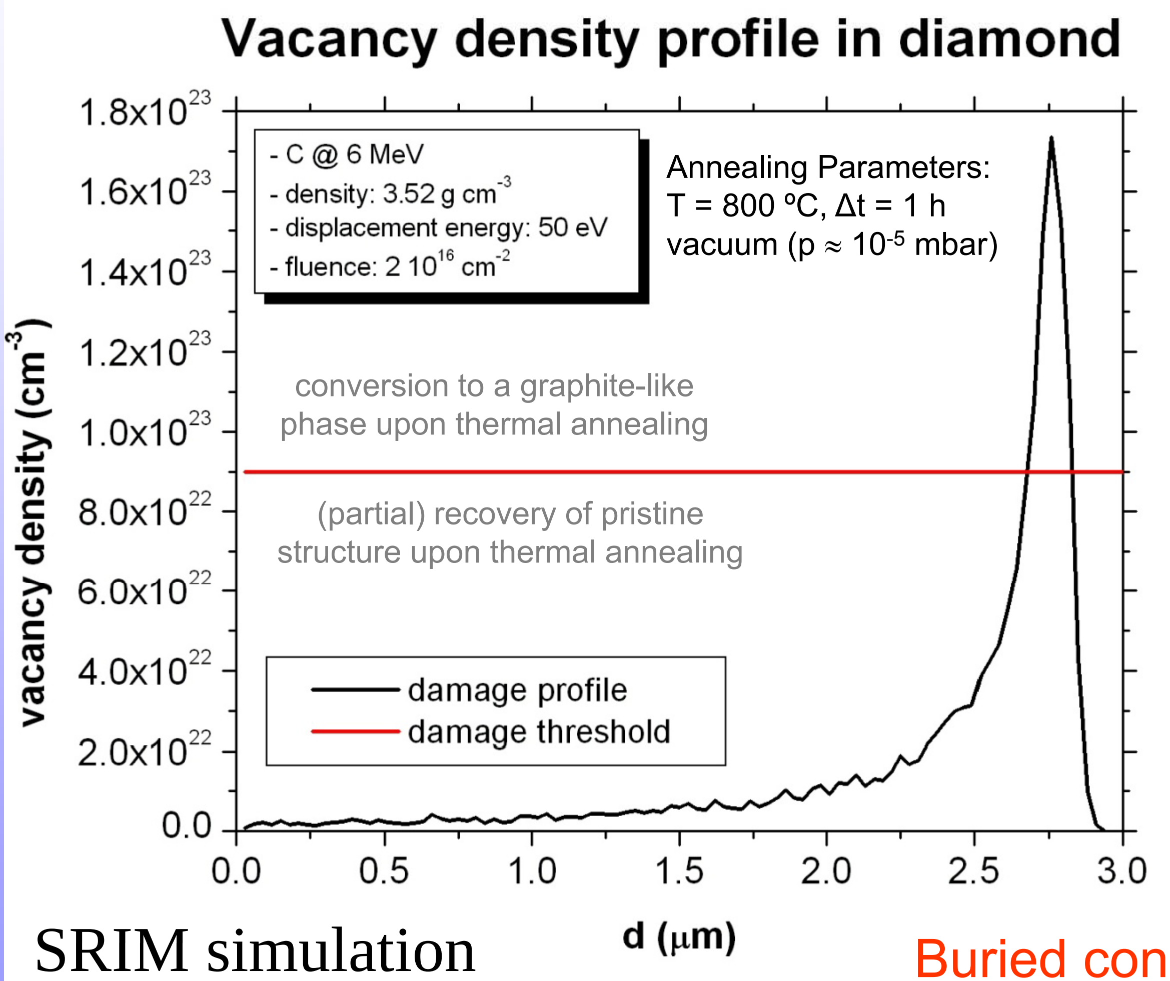

SRIM simulation

Interaction of MeV ions with matter results in structural damage.

Damage profile in diamond is shown in Fig and has a high peak at ~**2.7**μm under surface

Red line indicates damage threshold .

Buried conductive channel is obtained!

The damage threshold indicates the damage density above which the damage layer converts to graphtie after annealing. And below which the damage region recover to diamond after annealing.

How to make channels?

The procedure consist of four main stages:

a) evaporation of Cr-Au adhesion layer
b) deposition of semi-spherical Au contact mask
c) implantation with scanning ion microbeam
d) mask removal

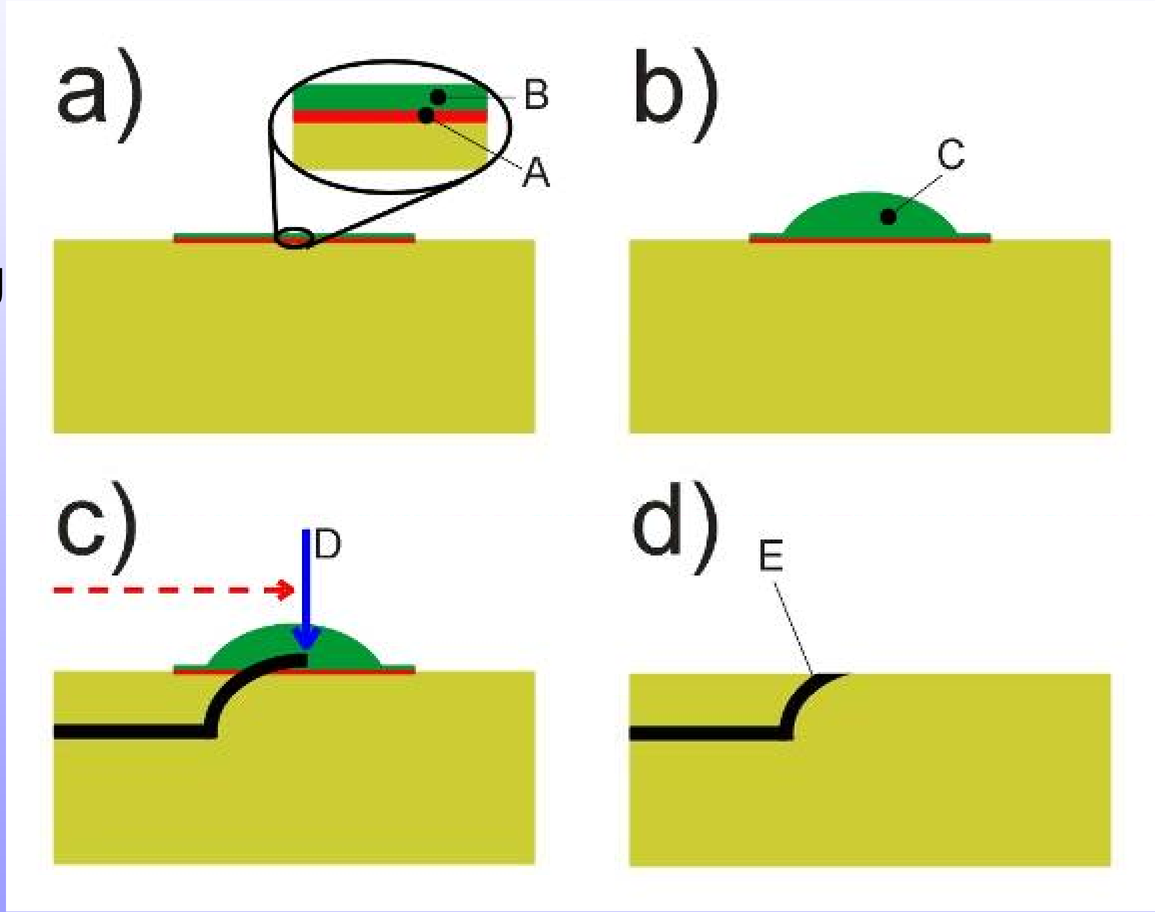

Notations in Figure:

Yellow: diamond
Green: Au layer (B), Au contact mask (C)
Red: Cr layer (A)
D: traectory of scanning ion beam
E: buried channel

And in this way the graphitic layer emerge at the surface.

Sample "1" fabrication

Sample (d_hpht_06, I5)

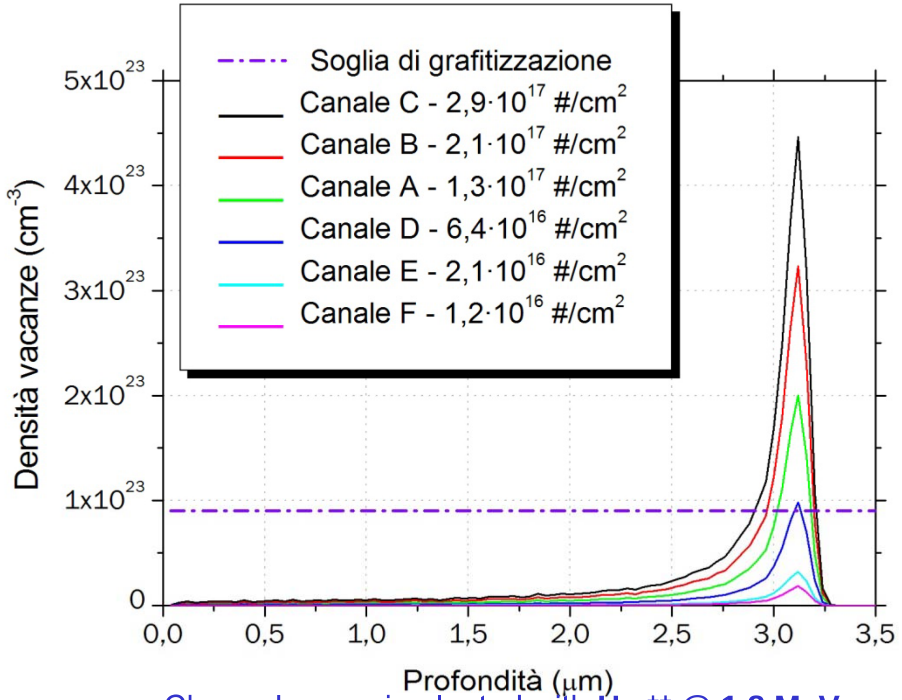

Channels were implanted with **H e^{++} @ 1,8 MeV at Laboratori Nazionali di Legnaro**

There are damage profiles created with different fluences in Fig. Channels A, B, C have peak of vacancy density above graphitization threshold, while channels D, E, F have they below this threshold.

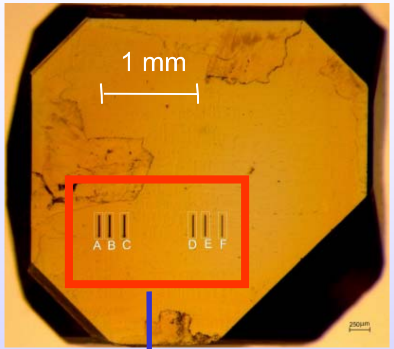

On the left side there are the Optical picture of synthetic single crystal diamond, And below magnified view of the channels.

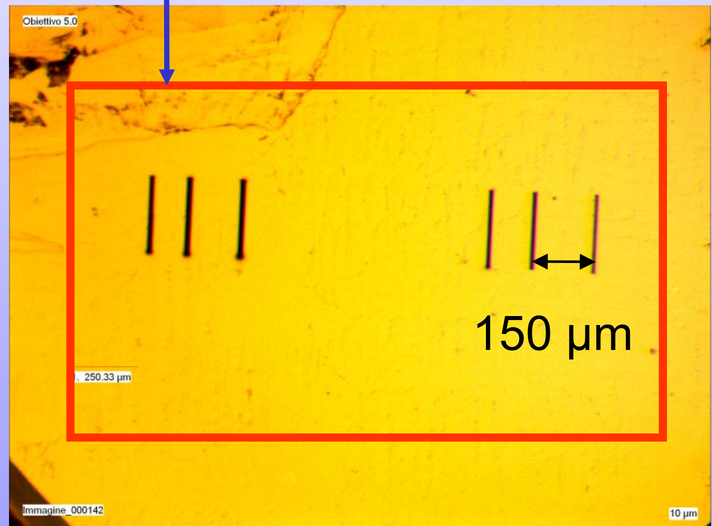

Sample was produced with high pressure high temperature (HPHT) method.
Crystal was cut along the (100) direction,
Ib Homo diamond.

AFM measurements

The charachterisation of the channel was done by AFM

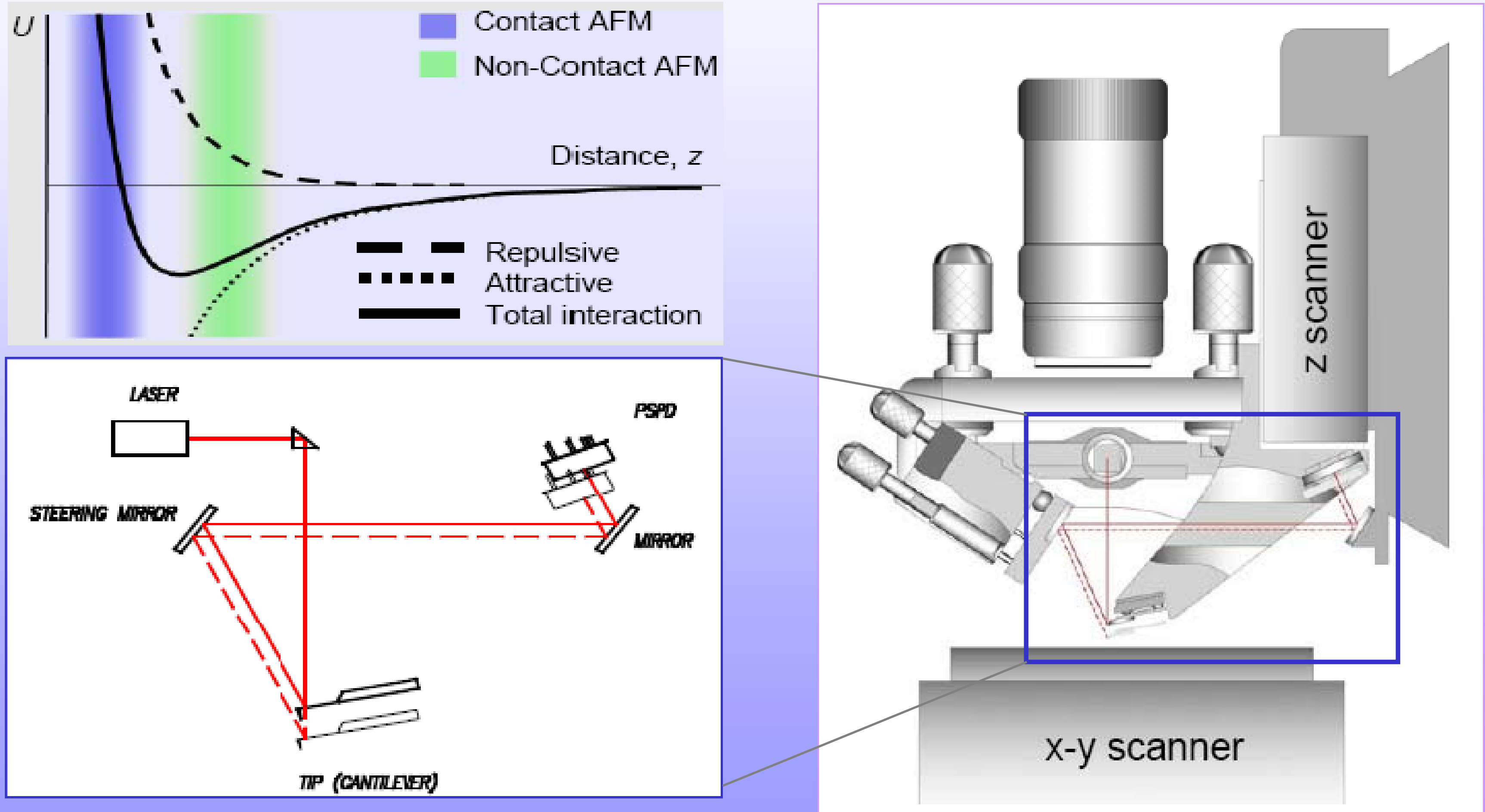

Morphological characterization of swellings of Sample “1”

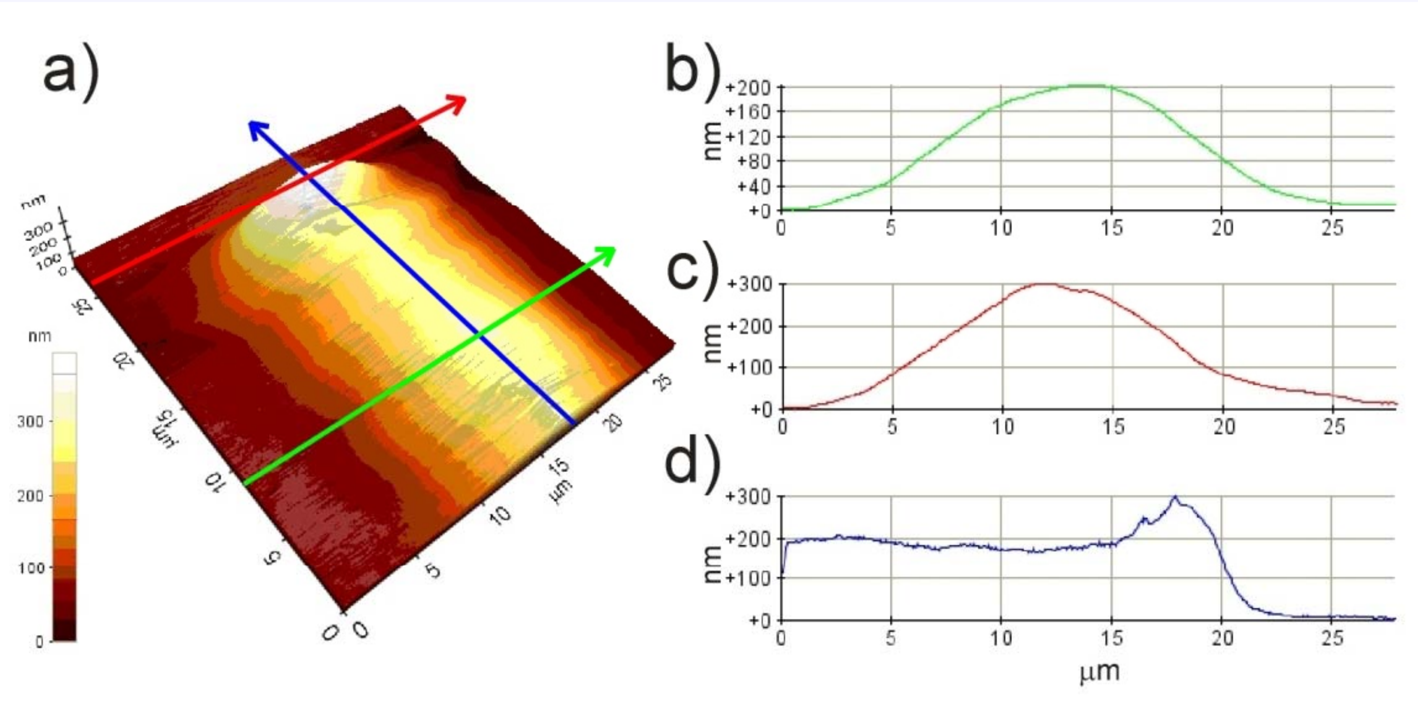

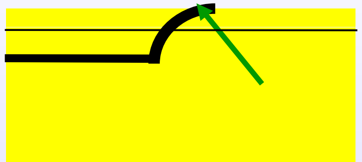

The morphology map for the buried channel and its end part is shown. Different profiles can be obtained depending on distance from the endpoint.

The swelling appears on surface due to the fact that the density of damaged volume has a smaller value than that of surrounding diamond material.

Morphological characterization of swellings Sample "2"

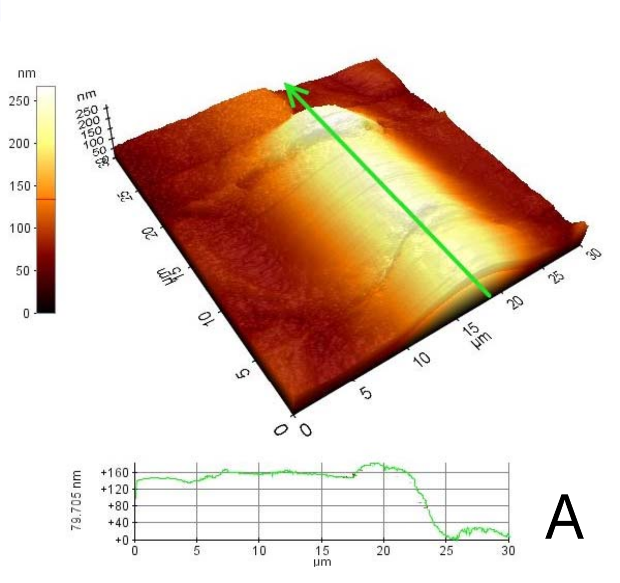

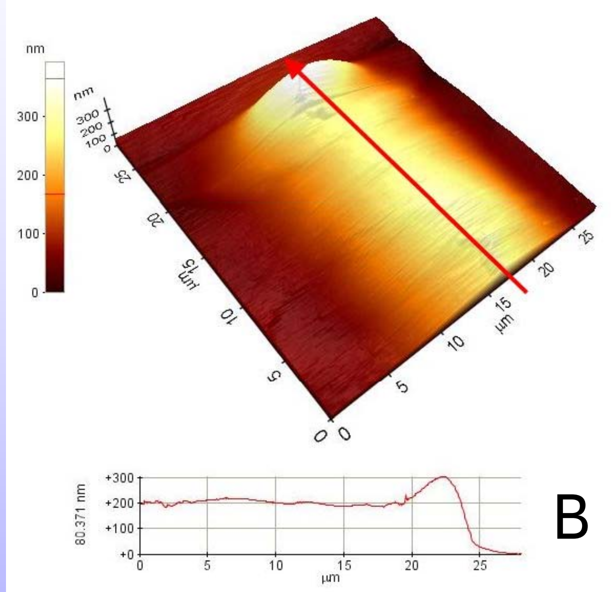

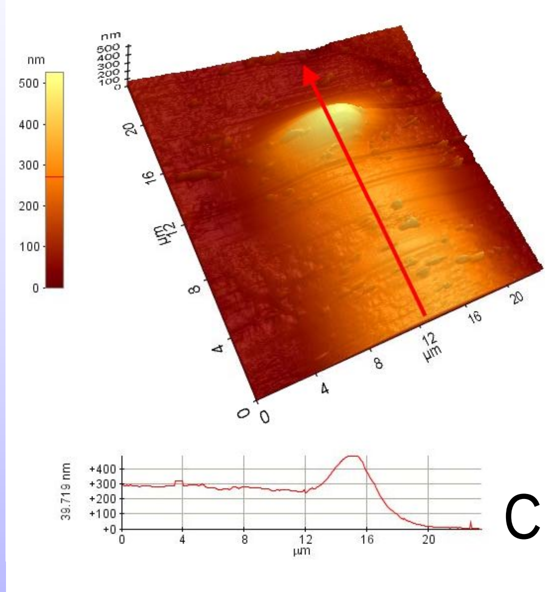

canale	fluence (cm^{-2})	channel (nm)	End channel (nm)
A	$1{,}3 \cdot 10^{17}$	160	200
B	$2{,}1 \cdot 10^{17}$	200	300
C	$2{,}9 \cdot 10^{17}$	300	480

The morphology maps of the implanted channels (A, B, C) show the profile of channel and its end part. Observed swelling at the endpoint of channel considered a fingerprint of the emerging channel.

Sample "2" description and swellings characterization

(d_hpht_06)

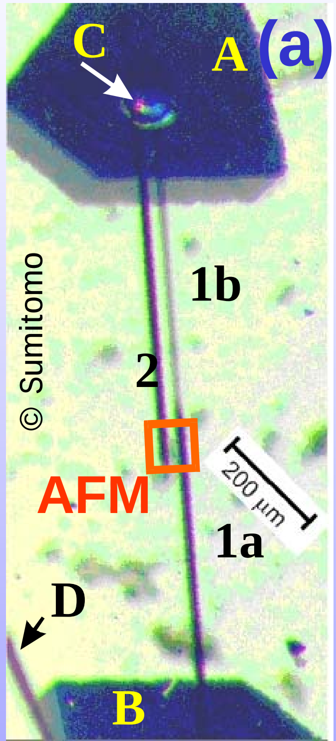

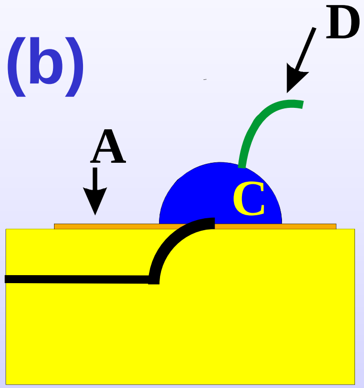

(a) Optical image of Sample 3 is 3×3×1.5 mm^3 single crystal diamond produced by HPHT method. The sample is cut along (100) direction.

(b) side view: C - semi-spherical gold contact, A – Cr-gold (Cr:10 nm) adhesion pad, B - Au (60 nm) pad, D - contact wire. Contacts were deposited before implantation. The black lines are implanted channels.

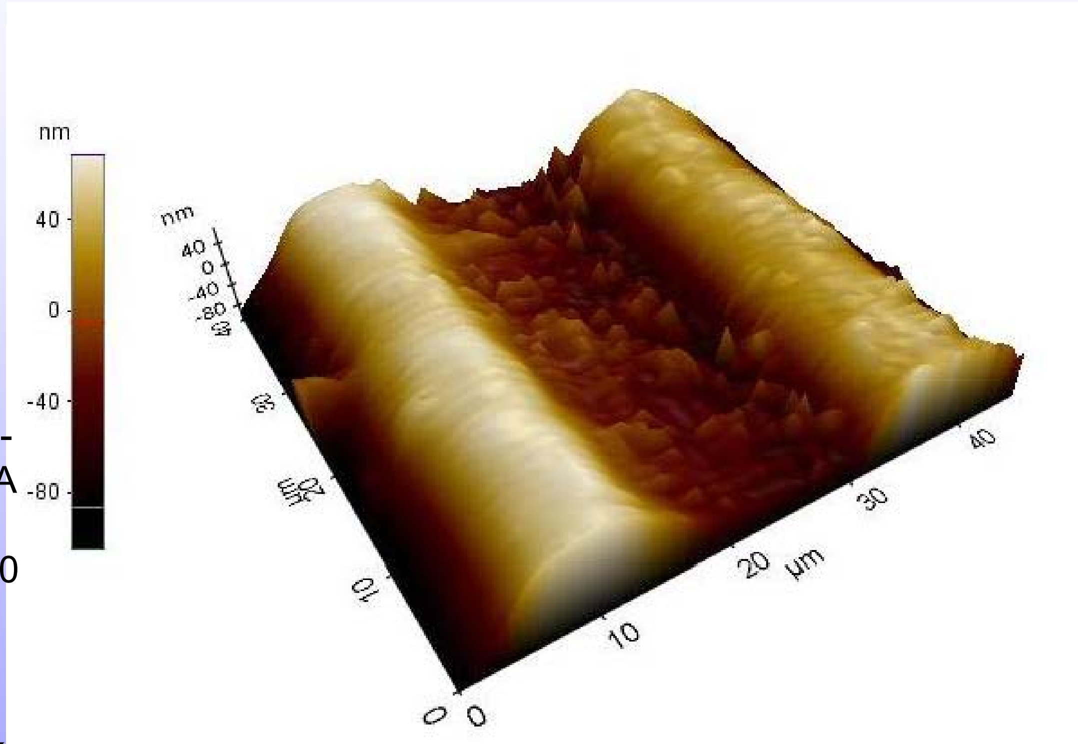

AFM morphology map of the region hightlighted with red square in optical image of the sample.Two parallel swellings related to respective channels are clearly observable

EFM of Sample “2”

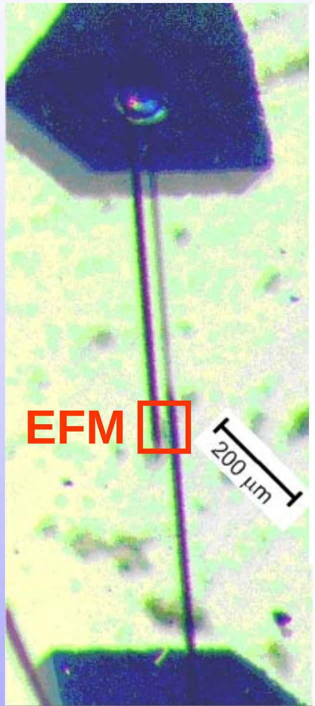

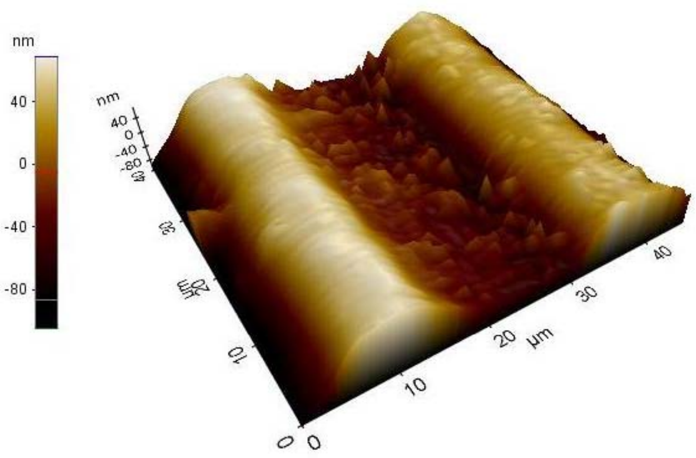

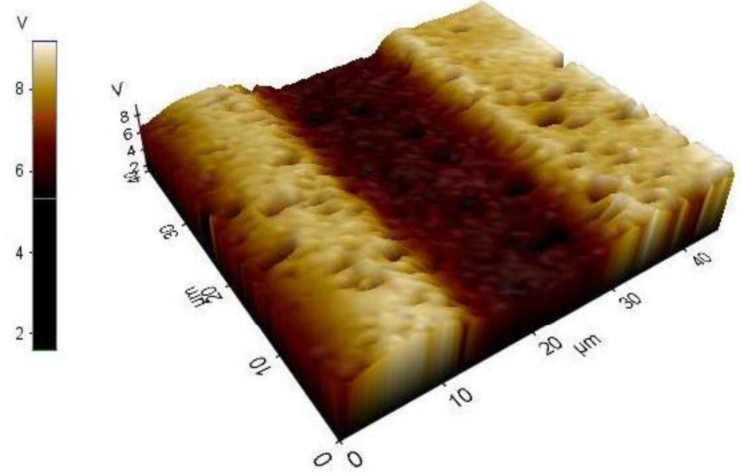

AFM height image of the central region marked with red rectangle

EFM amplitude map (right side) from the same region and profile of it; tip bias= -3.24 V.

Electrical characterization

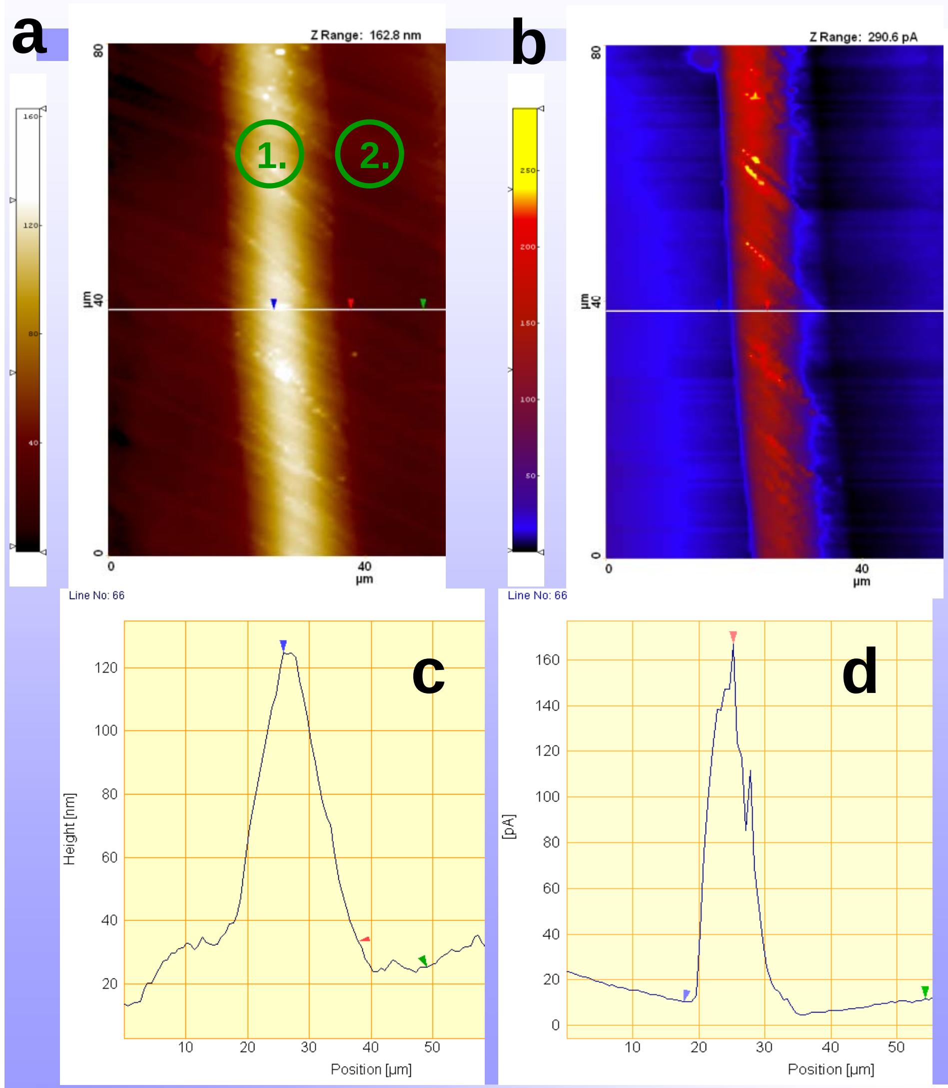

Sample 2 (not annealed) - single channel characterization. Height map **(a)** and corresponding Current map **(b)** where Sample Bias voltage is +10V. Cross-sections of channel marked with white lines showed separately as Height cross-section **(c)** and Current cross-section **(d)**. IV curves measured at point “1” **(e)** and those at point “2” **(f)** corresponds to channel and rest of the surface, respectively

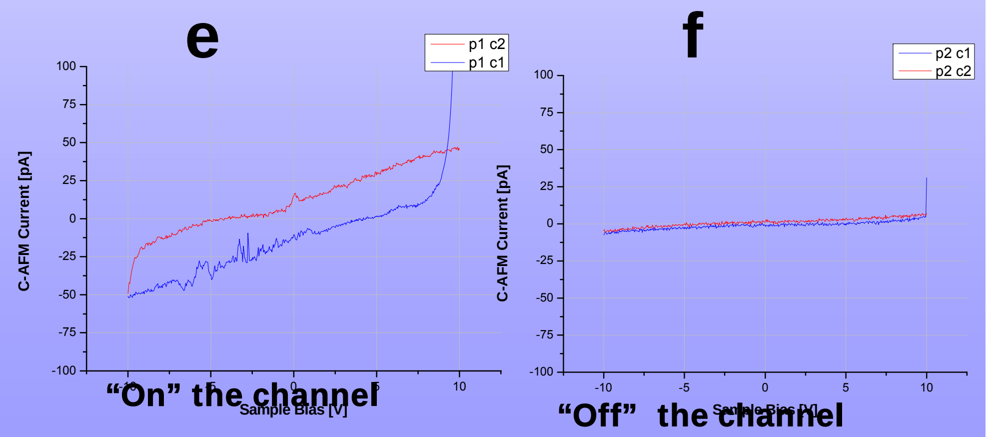

Electrical characterization (2)

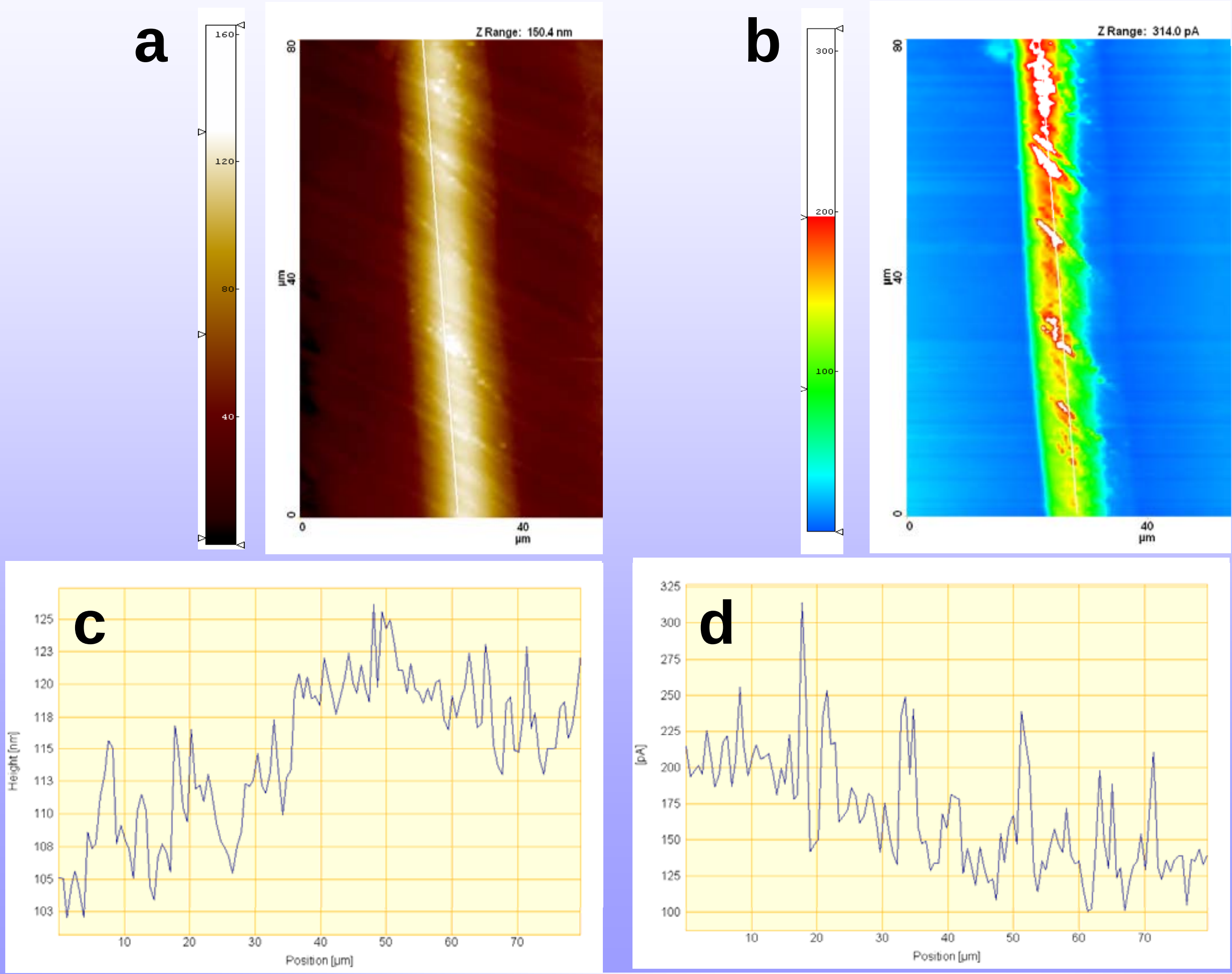

Sample bias applied +10V

Topography (a) map and Current map (b) of the channels (top images) and cross-sections along the white lines of the maps, (c) and (d) respectively

Conductivity of cap layer

Cap layer over the channel is produced with help of **Variable thickness mask**. This mask allows to tune the penetration depth of the ions.

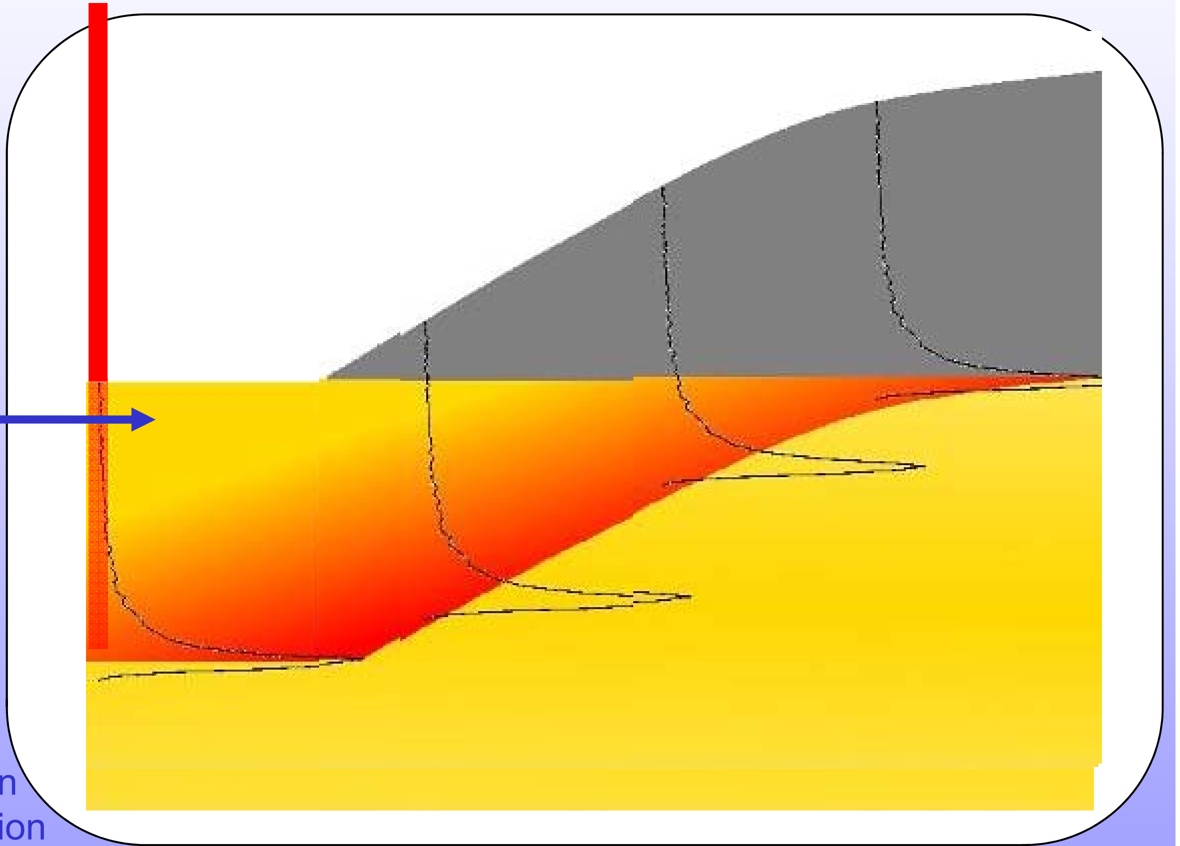

direction of scanning

1. After implantation of the channel the cap layer is conductive

Notations in Figure:
Yellow: diamond
Grey: Au contact mask **Red:** Ion beam, **Orange**- continius variation damage profile
Black: damage density profiles

2. After annealing, the conductivity of cap layer disappears

Optical characterization

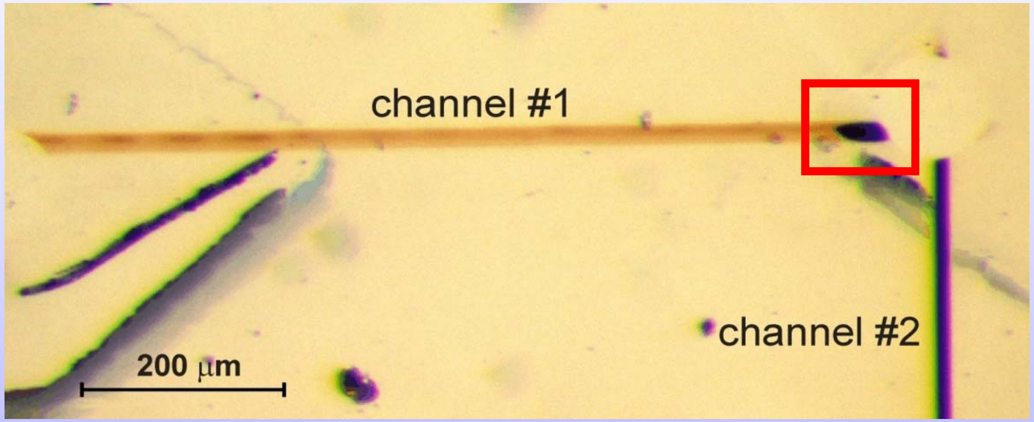

Channel 1 before (upper image) annealing and after annealing (lower image)

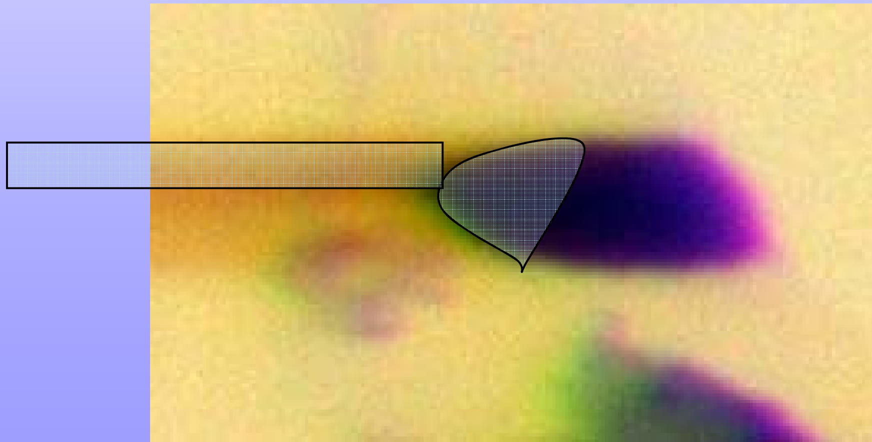

Magnified image of the place marked with red rectangle in Fig.3.20. Buried channel showed with a bar and its end at surface (contact place) with an ellipsoid

Electrical characterization

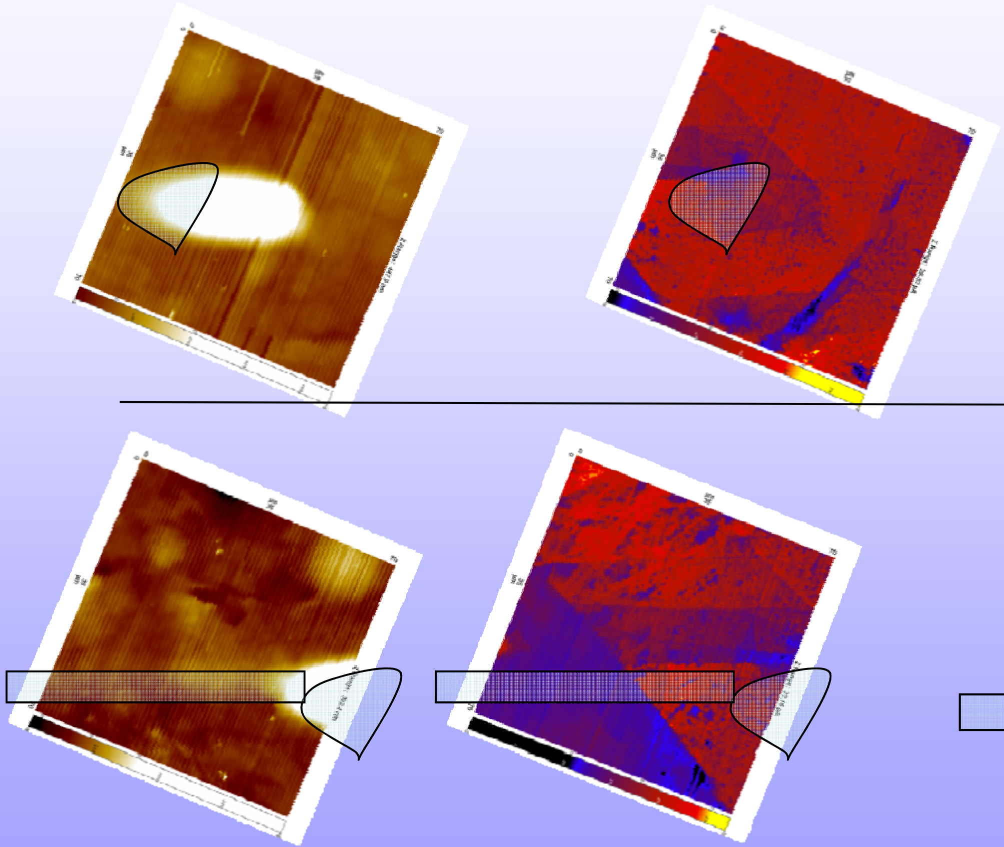

EFM maps of the area shown in Fig.3.21, describing absence of conductivity of channel 1 on d_hpht_01 sample after annealing: height (a) and current (b) maps of endpoint region, height (c) and current (d) maps of channel

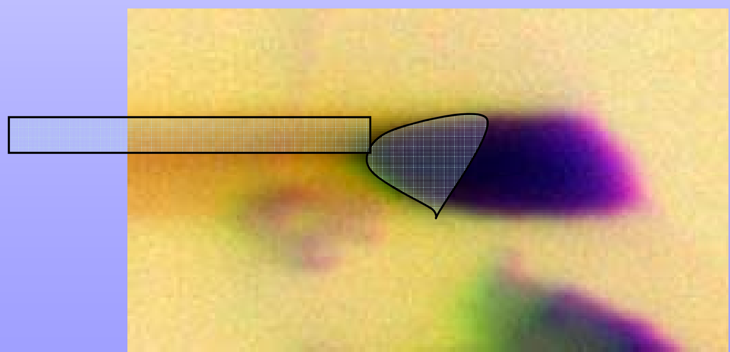

Conclusions 1

- Swelling of the surface due to ion implantation
- Evidence of channels emerging at the surface
- Evidence of conductivity of the cap layer
- After annealing the cap layer conductivity disappears

Conclusion

The scheme of diamond-based biosensor is presented. This scheme serves as a goal for development of different components of integrated biosensor device.

In this study in order to characterize the morphology and electrical features of MeV ion implantation channels has been preformed. The experimental evidence that the residual damage in diamond influence the conductivity of the buried channels, which disappears after annealing has been obtained.

Thank you for your attention!

Acknowledgments:

- Prof.Ettore Vittone
- Dr. Paolo Olivero
- Dr. Hao Wang
- Federico Picollo

This work was made possible thanks to support from Region Piedmont (Project D14 “Biosensori e interazione neuroni-superfici nanostrutturate”), and due to financial contributions from the Nanostructured Interfaces and Surfaces (NIS) centre of Excellence and from the ASP (Associazione per lo Sviluppo Scientifico e Tecnologico del Piemonte)

http://science.howstuffworks.com/diamond-pictures.htm

Samples

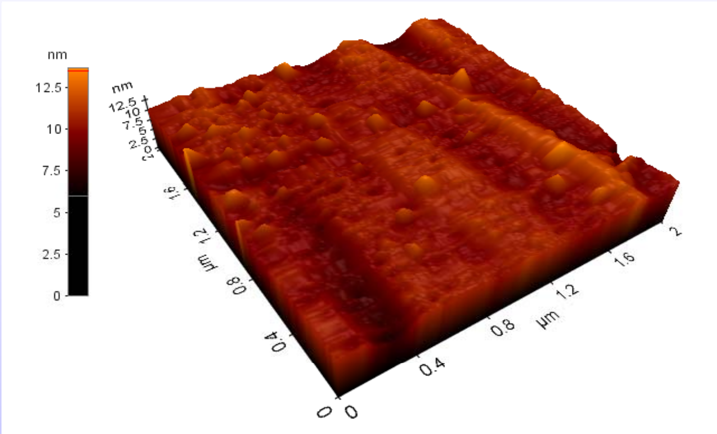

HOMO surface

Scheme of a typical sample

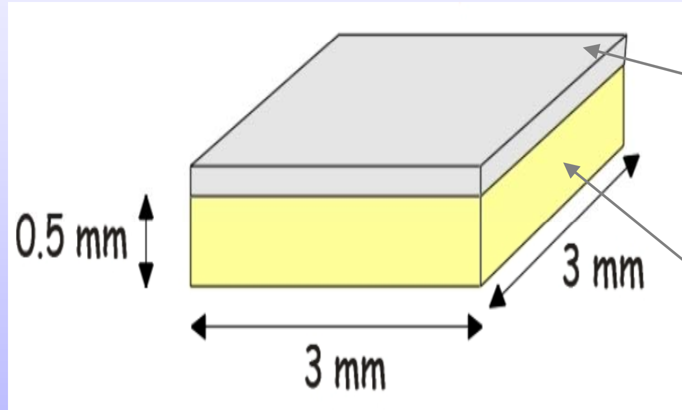

Active layer (0.3 –5 µm): HOMO IIa diamond

Substrate (0.5-1mm): HPHT Ib diamond (100)

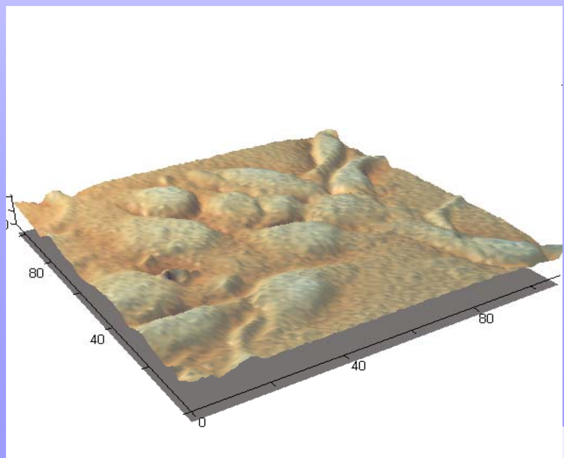

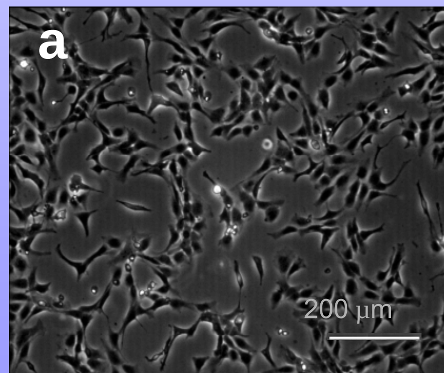

Electrostatic Force Microscopy

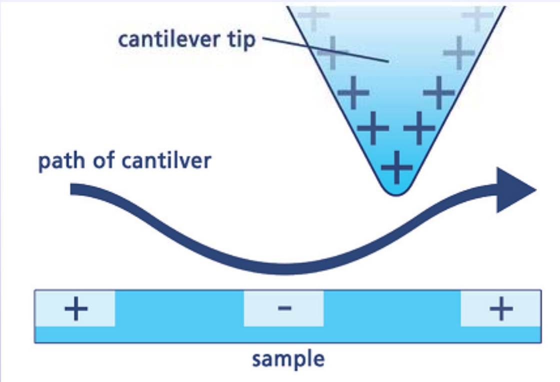

Scheme of EFM measurement

EFM characterization allowed to obtain data about local surface potential distribution

Electrostatic force microscopy (EFM)
applies a voltage between a conductive tip and the sample, with the cantilever hovering above the surface.

At such distances the deflection of the cantilever in variation with electrostatic forces over static charges is dominant with respect to the signal due only to topography. EFM then plots the locally charged domains of the sample surface (Fig.).

Electrostatic force microscopy has its application in the study of spatial variations of surface charge carrier density.